DRAG REDUCTION IN SEAWATER BY POLYMER ADDITION INTO A ROTATING CYLINDRICAL DOUBLE GAP DEVICE: EFFECT OF REYNOLDS NUMBER, POLYMER CONCENTRATION, AND SEA SALT CONCENTRATION

Rafhael Milanezi Andrade
Edson José Soares
Department of Mechanical Engineering, Universidade Federal do Espirito Santo, Avenida Fernando Ferrari, 514, Goiabeiras, 29075-910, ES, Brazil.
rafhaelmilanezi@gmail.com and edson@ct.ufes.br.

Abstract. Drag reduction by the dilute addition of high–molecular weight polymers in a turbulent flow has been extensively studied since the phenomenon was first observed over 60 years ago. Over the years reducers in flow systems have been successfully applied and represent a great potential benefit to many industrial processes. However, the phenomenon is not completely understood and many aspects of the problem remain unclear. Some important issues are related to the development of turbulent structures after the additive injection and to the breaking of the polymer molecules. These two phenomena impose a transient behavior on the polymer efficiency. Over time, at the very beginning of the test, drag reduction (DR) assumes a minimum value (sometimes negative) before reaching its maximum efficiency. When the degradation becomes important, DR starts to decrease until it achieves its asymptotic value, a time in which the polymer scission stops and the molecular weight distribution reaches a steady state. In the present work we study the drag reduction development from the very beginning of a turbulent flow into a rotating cylindrical double gap device. The DR is induced by three different polymers: Polyethylene Oxide (PEO), Polyacrylamide (PAM) and Xanthan Gum (XG). The first two are known as flexible molecules while the last one is considered rigid. The tests are conducted for a range of Reynolds number, polymer concentration, and synthetic sea salt concentration. The goal here is analyze drag reduction over the time using synthetic seawater as solvent. We observe that, when sea salt is present in the solvent, the onset of drag reduction occurs at higher Reynolds number and has significant influence on the extent of drag reduction in PEO and XG solutions.

Keywords: Turbulent flow, Drag reduction, Seawater, Double gap device.

1. INTRODUCTION

Polymeric drag reducers have been successfully used in a number of applications for more than 60 years (see Fabula (1971), Burger and Chorn (1980), and Golda (1986)). Over the years, researchers have been successful in analyzing this phenomenon and many remarkable papers with practical interest can be found (see Virk et al. (1967) and Virk (1975a), and Moussa and Tiu (1994)). Up to now, there has been no generally accepted theory for the mechanism of drag reduction, despite the fact that many researchers have contributed with some very significant papers (see Lumley (1973), Tabor and de Gennes (1986), and Dubief et al. (2004)). White and Mungal (2008) is a good review of some recent progress in understanding the fundamentals of polymer drag reduction.

The drag reduction phenomenon is very dependent on the kind of drag reducer used. Commonly, fibrous particles, surfactants and polymers are used. These last are very far more efficient and have been widely analyzed over the years. Concerning their mechanical resistance, polymers can be divided into flexible and rigid molecules. The former are generally of high molecular weight with a linear chain, among which Poly(ethylene oxide), Polyacrylamide and Polyisobuthylene are examples which have been extensively tested over the years (see Virk et al. (1967), Paterson and Abernathy (1970), Virk (1975b), Kalashnikov (1998), Kalashnikov (2002), Choi et al. (2001) and Bizoto and Sabadini (2008)). A huge disadvantage, which is a great obstacle to the practical use of flexible polymers is their mechanical degradation. A possibility that deserves our attention is the use of polysaccharides such as Hydroxypropylguar, Gar Gum and Xanthan Gum (see Kim et al. (1985) and Chakrabarti et al. (1991)). Such molecules are rigid and much less susceptible to mechanical scission. The main problem in this case is the biological degradation, though it is much less accelerated when compared to the mechanical scission.

Among the different rigid polymers known in the literature, Xanthan Gum seems to be of particular practical interest in food, pharmaceutics, cosmetics, and the oil industry, in which it is widely used as a drag reducer in drilling well operations. From the molecular point of view, XG possesses a linear main chain of (1-4)-β-D glucose, similar to cellulose, with a trisaccharide side chain on every second D-glucose (see Bewersdorff and Singh (1988) for details). In fact, such a complex structure is responsible for its rigidity and stability. Its structure is highly dependent on the temperature and salinity. At moderate temperatures and low ionic forces, XG presents a stable organized helical conformation resulting in a rigid molecular structure, as reported by Morris (1977) and Norton et al. (1984). Such an organized structure can be modified by increasing temperature or salinity. In such conditions, the ionic forces are

altered and the helical configuration changes to a recoiled one. In this new configuration, the Xanthan Gum's capability to reduce drag drops dramatically. In fact, temperature plays a complex role in the structural configuration of XG. Below a certain value of T, known as the *transition-midpoint temperature*, an increase in T causes an increase in the mean molecule length, keeping the helical structure stable as suggested by Sohn et al. (2001). The salinity also plays a very important role in the structural configuration of XG. For more details of the mechanism and dynamics of XG's structure, see Morris (1977) and Norton et al. (1984).

A huge obstacle to obtain an accepted theory of the phenomenon of drag reduction is the mechanical molecular degradation. This issue involves a strong interdisciplinary connection between chemistry and fluid mechanics. This issue has received deserved attention over the years and many aspects of the problem have been studied, such as the effect of concentration, molecular weight, Reynolds number and temperature on the efficiency of drag the reduction (see Paterson and Abernathy (1970), Moussa and Tiu (1994), and Pereira and Soares (2012)). Using an experimental turbulent pipe flow apparatus, Vanapalli et al. (2005) performed some careful analyzes to show that drag reduction, DR, decreases as a consequence of polymer degradation but reaches a steady state after a certain number of passes through the pipe flow apparatus. In other words, the molecular scission stops after a long enough time. This tendency is supported by many other results, such as those reported by Nakken et al. (2001), Choi et al. (2001), Kalashnikov (2002), and Pereira and Soares (2012).

The dependence of drag reduction on time is not exclusively related to molecular degradation. As reported by Dimitropoulos et al. (2005), the turbulent structures take some time to rearrange following a polymer deformation and the DR does not achieve its ultimate level instantaneously. In fact, DR is a complicated function of time. Figure 1 shows schematically the development of a polymer induced near-wall drag reduction, defined as $DR = 1 - f_p / f_0$, where f_p is the friction factor of the polymeric solution and f_0 that of the solvent. This kind of figure can be constructed by monitoring the drag reduction along a pipe or channel after the polymer injection or by using any rotating apparatus. The last strategy is evidently easier. As sketched in Figure 1, the available results concerning flexible polymers suggest that at the very start of the test, DR decreases from DR to $DR_{\min}$ before achieving its top level of efficiency, $DR_{\max}$. Since polymers extract energy from the vortices and release energy to the mean flow in a coil-stretch cycle, we presume that the maximum drag reduction occurs when a sufficient number of the molecules are in this coil-stretch cycle (Dubief et al. (2004)) and a state of equilibrium with the turbulent structures has been achieved. We will refer to the time to achieve $DR_{\max}$ as the developing time, denoted t_d. The increasing friction factor at the beginning of the process is related to an instantaneous increment of the local extensional viscosity after a high polymer stretching. Following t_d, we observe a constant value of DR for a period of time, which is denoted by t_r, the resistance time. Finally, after this period, DR begins to fall, reaching a minimum level after a long enough time, when the degradation process has reached its steady state and DR assumes an asymptotic value, DR_{asy}. The time to reach DR_{asy}, t_a, is relatively large compared with the stretching time of a single molecule, because the molecules are stretched and degraded step-by-step (see Elbing et al. (2011)). Thus, we could presume that during t_r the increasing number of molecules in the coil-stretch cycle is balanced by the molecular degradation, and the ultimate level of drag reduction is sustained. Following that, with a continuous degradation, the turbulent structures depart from their equilibrium and start to increase until achieving the final steady state in which the level of drag reduction assumes a constant value, DR_{asy}.

There has been a number of papers studding the effect of molecular conformation on drag reduction by changing the interactions between polymer molecules and solvent. Hershey and Zakin (1967) observe that the drag reducing ability of polyisobutylene is better in a good solvent (cyclohexane) than in a poor solvent (benzene). They indicate that good solvents allow the polymer molecules to expand more freely in the solution; on the other hand, in poor solvents the molecule's volume is smaller. Later, Zakin and Hunston (1978) report that poor solvents affect the mechanical degradation of polymers. They found that in a poor solvent, mechanical degradation is more rapid than in a good solvent. Experimental analysis conduced by Hunston and Zakin (1980) also show that the onset of drag reduction occurs earlier when polymer molecules is dissolved in a better solvent.

Many practical applications of drag reduction require specific studies with seawater, for example, in ocean thermal energy conversion (OTEC) system (Choi et al. (2001)), in ocean transport ships and submarines (Elbing et al . (2009)), among others. Despite the potential use, little research has been done to study the drag reduction in such conditions. Experimental results obtained by Elbing et al. (2009) e Kamel et al. (2009) in a pipe flow apparatus, evaluate the effect of sea water in the drag reduction. They note that the sea water delays the onset of drag reduction and reduces the polymer efficiency in relative to the pure water solvent solutions. However the authors did not evaluate the polymer efficiency over the time and do not perform specific tests to analyze the extend of polymer degradation in salt solutions. There are also no data comparing the effect of seawater in different polymers. In view of these issues, in the present paper we study the drag reduction over de time into a rotating cylindrical double gap device using synthetic seawater as a solvent. The experiments were conducted for a range of Reynolds number, polymer concentration, and synthetic sea

salt concentration for Poly(ethylene oxide) (PEO), Polyacrylamide (PAM) and Xanthan Gum (XG) in an attempt to understanding the effect of seawater on the drag reduction and polymer degradation over the time.
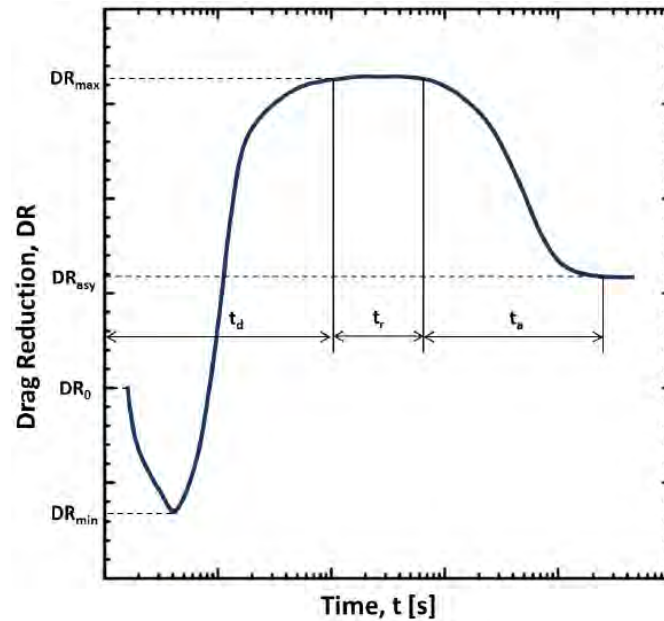

Figure 1. Sketch of the evolution over time of the polymer-induced drag reduction.

2. EXPERIMENTAL APPARATUS AND PROCEDURE

The majority of the experimental results on drag reduction by polymer additives available in the literature have been obtained for pipe flow systems, obviously, because they are widely used in many industrial transport processes. However, the use of pipe systems to analyze drag reduction is extremely difficult and time consuming. A way to overcome this difficulty is by using a rotational apparatus, such as coaxial cylinders (Kalashnikov (1998) and Kalashnikov (2002)), a rotating disk (Choi et al. (2001)) or a double-gap cylindrical geometry (Nakken et al. (2001), Bizotto and Sabadini (2008), and Pereira and Soares (2012)). This last geometry has a large contact area, which provides measurements with a quite good accuracy, even for small values of the Reynolds number. Recently Pereira and Soares (2012) used this kind of apparatus, shown in Figure 2, to obtain their results.
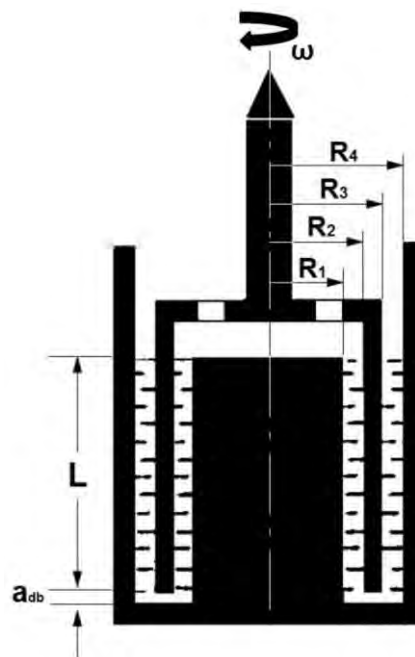

Figure 2. The axial symmetric double gap geometry.

The tests were carried out using a commercial rheometer, model Haake Mars II, manufactured by Thermo Scientific, Germany. The sample was located between the two rigidly interconnected coaxial and stationary surfaces, which have an axial symmetry. The rotor is a thin-walled coaxial tube located between these two fixed cylindrical surfaces which can rotate over the sample holder's axis of rotational symmetry at a given angular velocity. The radii $R_1 = 17.75$ mm, $R_2 = 18.00$ mm, $R_3 = 21.40$ mm, and $R_4 = 21.70$ mm, and the rotor height $L = 55.00$ mm, shown in Figure 2, are the important scales of our test section. The sample volume is 6.3 ml.

For a given angular velocity (ω), the mean shear rate ($\dot{\gamma}$) is determined by Eq. (1) as a function of the rotation speed of rotor, n, and $K = \frac{2R_4{}^2}{R_4{}^2 - R_3{}^2} = \frac{2R_2{}^2}{R_2{}^2 - R_1{}^2}$, a geometrical factor:

$$\dot{\gamma} = K\omega = K\frac{2\pi}{60}n$$

(1)

The measured torque on the rotor is related to the nominal shear stress, τ, by Eq. (2):

$$T = \frac{4\tau\pi L\left(\delta^2 R_3{}^2 + R_2{}^2\right)}{1 + \delta^2}$$

(2)

Here, $\delta = R_4/R_3 = R_2/R_1$ is the aspect ratio. Thus, we can calculate the Fanning friction factor based on the characteristic radius, which is given by the mean radius ($\bar{R} = \frac{R_2 + R_3}{2}$):

$$f = \frac{2\tau}{\rho u^2} = \frac{2\tau}{\rho\left(\omega\bar{R}\right)^2}$$

(3)

The Reynolds number is defined by Eq. (4):

$$\text{Re} = \frac{\rho\bar{h}u}{\eta} = \frac{\rho\bar{h}\left(\omega\bar{R}\right)}{\eta}$$

(4)

where η is the solution's viscosity, $\omega\bar{R}$ is a characteristic velocity and $\bar{h}$ is the average gap given by $\bar{h} = \frac{(R_2 - R_1) + (R_4 - R_3)}{2}$.

In order to classify the distinct flows in the double-gap geometry, for a range of analyzed Reynolds numbers, we used the Taylor number given by Eq. (5).

$$T_a = \frac{\bar{R}\bar{h}^3\omega^2}{\nu^2}$$

(5)

where ν is the cinematic viscosity.

We tested solutions of Poly(ethylene oxide), Polyacrylamide, and Xanthan Gun. The molecular weight of the first and second materials is $M_v = 5,0 \times 10^6$ g/mol, whereas that of the last one is $M_v = 2,0 \times 10^6$ g/mol. All our chemical supplies were provided by Sigma–Aldrich. We obtained the molecular weight by calculating the intrinsic viscosity, $[\eta]$, using the Huggins equation (for details see Flory (1971)) and our measurements were very close to the values quoted by Sigma-Aldrich. The measured intrinsic viscosity, $[\eta]$, was also used to estimate the overlap concentration for PEO and PAM by means of the relation $c*[\eta] = 1$. For the PEO solutions, the calculated value was $c* = 3125$. For the PAM, the overlap concentration was around $c* = 100$ ppm. This procedure was not used for the XG solutions, as it is highly shear-thinning. An attempt to obtain the overlap concentration of this polymer was conducted by measuring its zero-shear viscosity at different concentrations. There is a value of concentration for which the variation of η_0 is considerably increased, and we suppose that the overlap concentration, $c*$, is below such a value. We conducted here the same procedure used by Jaafar et al. (2009). By means of this technique, we estimated the overlap concentration of the Xanthan Gum to be $c* = 940$ ppm. The maximum polymer concentration used in this work was 100 ppm which suggests we are working with diluted solutions. The polymer powders were gently deposited on the solvent surfaces

(deionized water or synthetic seawater). Each test was carried out after 24 hours, time for complete natural diffusion. This procedure was adopted to avoid any polymer degradation before the beginning of the test.

The maximum rotational speed of the rotor used was $n = 3000$ rpm (revolution per minute). The flow field becomes unstable in T_a, Eq.(5), close to 1700. This value of T_a is achieved when n is close to 500 rpm. This corresponds to $Re \geq 350$. Drag reduction is only observed for values of T_a beyond this critical value. In the main tests, the rotational speed was kept constant to display the drag reduction as a function of time which was extended over 4000 seconds, time to achieve DR_{asy} in all tests, and around 4000 shear stress values were measured.

The kind of geometry used here can, eventually, exhibit some laminar instabilities, such as Taylor-vortices. Thus, someone could question whether our results are related to Taylor instabilities or to turbulence. In an attempt to quantify the real importance of laminar instabilities on the drag reduction and degradation, Pereira and Soares (2012) performed a sequence of tests using the double gap and a standard Taylor-Couette geometry for a range of Taylor numbers. The author's analysis conducted for flexible polymers showed that, the drag reduction and, principally, the degradation, in the double gap are predominantly related to turbulence instead of any kind of laminar instability.

3. RESULTS AND DISCUSSION

The results are displayed considering variations in the Reynolds number, polymer concentration, and synthetic sea salt concentration. Synthetic sea salt was tested in two concentrations for PEO and PAM solutions, 3,5% by weight (SSW) as Elbing et al. (2009) and 10% by weight (SSW 10%). In addition, one more salt concentration was testes for XG, 10ppm (SSW 10ppm). We present our results in three parts. In subsection 3.1, we show the Fanning friction factor in Prandtl-von Karman coordinates for a range of concentrations of each polymer and synthetic sea salt concentration. Subsection 3.2 presents DR over time from the very beginning of the test until reaching its asymptotic value after a long enough time. Finally, in subsection 3.3, we present the time dependent relative drag reduction, DR', for PEO solutions, which showed more clearly the influence of polymer degradation, where the loss of efficiency is more clearly discussed.

3.1 Fanning friction factor in Prandtl-von Karman coordinates

Figure 3 shows the Fanning friction factor for a range of polymer concentration, c, of PEO, PAM, and XG (Figure 3 A, C, E) and synthetic sea salt concentration (Figure 3 B, D, F) in Prandt-von Karman coordinates. In these tests the rotation speed was gradually increased from 0 to 3000 rpm over ten minutes and the temperature was maintained at 25ºC. We can observe for the flexible polymers (PEO and PAM) and also for the rigid one (XG), Figure 3 A, C and E that the friction factor falls and the onset of drag reduction occurs at smaller values of Reynolds numbers with increasing polymer concentration, as widely reported by a number of researchers (Hershey and Zakin (1967), Virk et al. (1967), Burger and Chorn (1980), Moussa and Tiu (1994), Vanapalli et al. (2005) and Pereira and Soares (2012)). It is also clear that the values of the coefficient $1/\sqrt{f}$ are more pronounced in the PEO solutions. The smallest values of this parameter are observed in the XG solutions. For PEO and PAM solutions, it is clearly observed that the curves at distinct concentrations are moving away from each other with increasing Reynolds number. In contrast, the lines displayed for each concentration of XG, after the onset, seem to be parallel. On the other hand, the onset of drag reduction occurs at a much smaller Reynolds number in XG solutions, easily perceived for c =50 ppm. This observation suggests that the Reynolds number plays a weak role in Xanthan Gum solutions, as reported by Bewersdorff and Singh (1988). The reason for these observations is related to the fact that XG is a rigid polymer and is already extended on its equilibrium state at rest. Hence, our observation is in agreement with the idea of a Type B mechanism of drag reduction reported by Virk et al. (1997). Concerning the effect of seawater, also in Figure 3 A, C and E we can see that, in all solutions with synthetic salt water (SSW, 3,5 % by weight), the onset of drag reduction is delayed, in other words, occurs at higher values of Reynolds numbers, as observed by Elbing et al. (2009) and Kamel et al. (2009). This effect is more evident in the more concentrated solutions c = 50ppm. We can also see that the effect of seawater is less important in PAM solutions. On the other hand, the XG solutions with salt are dramatically affected. Perhaps this is related to the change in molecular structure of XG, as reported by Morris (1977) and Norton et al. (1984). Comparing the results for different salt concentrations (Figure 3 B, D, F), we can see that the onset of drag reductions is delayed with increasing of synthetic sea salt concentration. In Figure 3 F only 10ppm of sea salt (0,001%) can completely change the efficiency of XG. The addition of more salt does not cause significant changes on the friction factor (dark gray and black circles). We can also see that the efficiency of PEO solution is significant affected by addition of higher amounts of salt (Figure 3 B). As reported by Hershey and Zakin (1967), Zakin and Hunston (1978), and Hunston and Zakin (1980), possibly the addition of this synthetic sea salt become the deionized water a poor solvent for PEO.
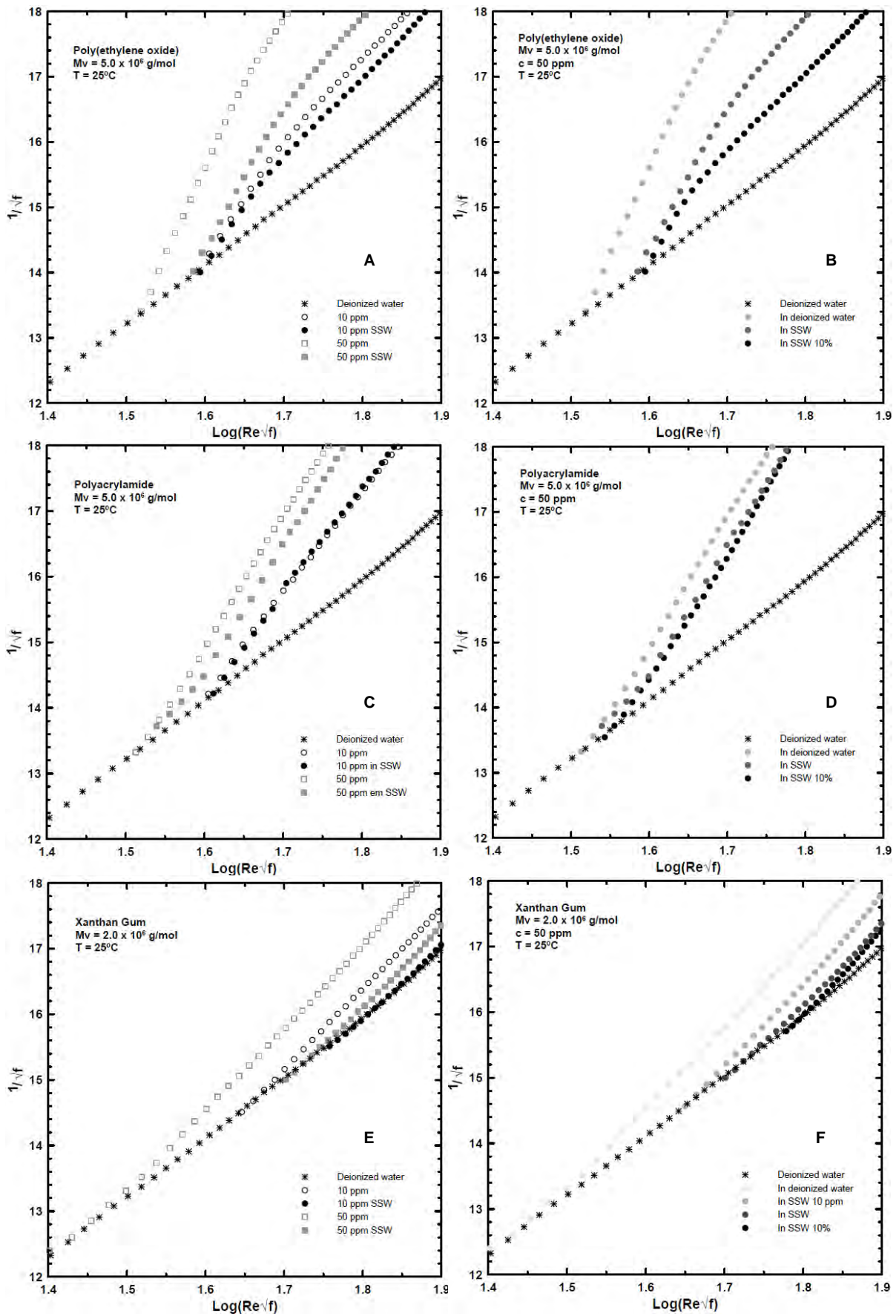
Figure 3. Effects of polymer concentration and synthetic sea salt concentration on Fanning friction factor, f, as a function of Reynolds number, Re.

3.2 Drag reduction decay

Figure 4 displays drag reduction against the time for a range of Reynolds number for PEO, PAM, and XG, $c =$ 50ppm, in synthetic seawater and deionized water. In these tests the rotational speed was kept constant to display the drag reduction as a function of time, which was extended over 4000 seconds, time to achieve DR_{asy} in all tests. The temperature was kept at 25ºC.
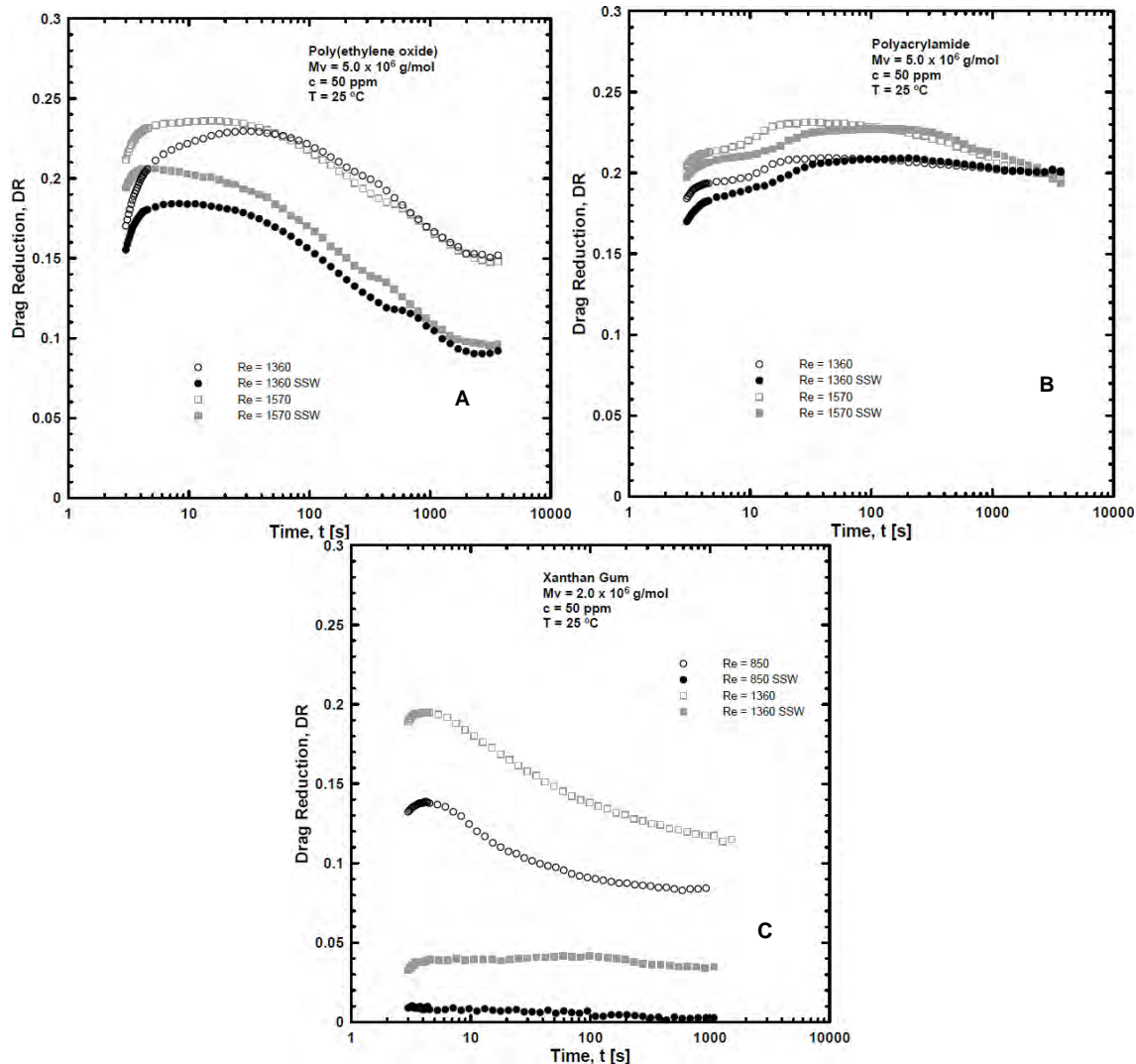

Figure 4. Effect of Reynolds number on DR as a function of time in synthetic seawater and deionized water.

We can note an increase of DR_{max} with increasing Re, as noted by Kalashnikov (1998), Sohn et al.(2001), and Pereira and Soares (2012) using a rotating cylinders apparatus. The maximum level of efficiency is sustained for a while, the resistance time, t_r. Supposedly, when the degradation becomes important, DR starts to decrease until achieving its asymptotic value, DR_{asy} a time during which the polymer scission stops and the molecular weight distribution reaches a steady state, as observe Nakken et al. (2001), Vanapalli et al. (2005), and Pereira and Soares (2012). Elbing et al. (2011) argue that the time to reach DR_{asy}, t_a, is relatively large compared with the stretching time of a single molecule, because the molecules are stretched and degraded step-by-step. It is interesting to observe that t_r is shorter in XG than the others polymers. Concerning the effect of seawater as a solvent, Figure 4 shows a large influence on extend of drag reduction by PEO. As seen in the curve of friction factor, drag reduction is lower in solutions with synthetic sea salt; the same effects are noticed by Elbing et al. (2009) and Kamel et al. (2009). In these conditions t_r and DR_{asy} are smaller, indicating that polymer degradation is more pronounced. We can also see that PAM efficiency is not significantly affected by synthetic seawater. On the other hand, the salt effect on the Xanthan Gum is more evident. An abrupt fall of efficiency is noted and, in $Re = 850$, DR is practically nil. We can clearly note a

Rafhael M. Andrade and Edson J. Soares
Drag Reduction in Seawater by Polymer Addition into a Rotating Cylindrical Double Gap Device

great difference between the XG solutions with deionized water (empty symbols) and seawater (full symbols). The development time, resistance time, and asymptote time, clearly perceived in solutions without salt, are no longer observed. Apparently the drag reduction starts at DR_{asy} in XG solutions with synthetic sea salt.

The effect of concentration of PEO, PAM, and XG on drag reduction as a function of the time in synthetic seawater and deionized water is displayed in Figure 5. In these testes Reynolds number (1360) and temperature (25°C) are fixed.
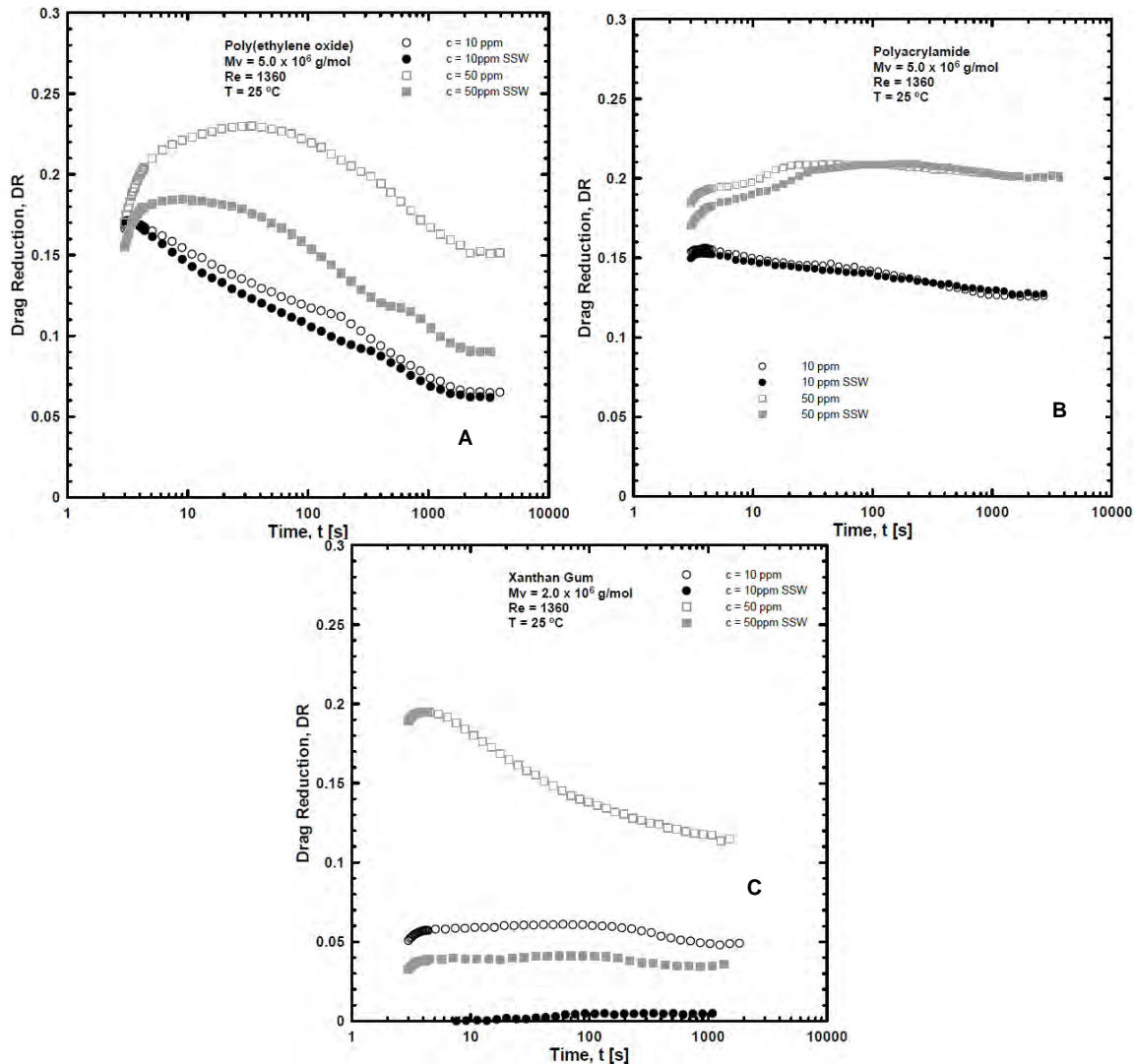

Figure 5. Effect of concentration, c, on DR as a function of time in synthetic seawater and deionized water.

We can observe that DR_{max} is an increasing function of concentration, as widely reported by a number of researchers (Hershey and Zakin (1967), Virk et al. (1967), Burger and Chorn (1980), Moussa and Tiu (1994), Vanapalli et al. (2005), and Pereira and Soares (2012)). The period of time that DR_{max} is sustained, t_r, increases with increasing polymer concentration. Pereira and Soares (2012) suggest that at high concentrations, the increased number of molecules per volume provides the ultimate level of drag reduction for a longer time and the decrease of DR is delayed for two reasons. The first, as reported by Elbing et al. (2011), is based on the hypothesis that the molecules are stretched and degraded step-by-step and consequently, the increased number of un-degraded molecules in higher concentrations can provide the vortex suppression for longer time. The second reason is possibly related to the fact that the extensional viscosity is an increasing function of concentration, as argue Merrill and Horn (1984). At higher extensional viscosity the extensional strain rate decreases and we suppose the degradation rate falls and contributes to delay the time when DR starts to decreases. Therefore the increase of concentration delays the degradation process, as noted by Paterson and Abernathy (1970), Moussa and Tiu (1994), and Sohn et al. (2001). Concerning the effect of seawater as a solvent, Figure 5 A and B shows that the effect of salt is less important in less concentrated solutions, $c = 10$ ppm. Similar effect is noted by Elbing et al. (2009). On the other hand, the curves of XG are significantly different from the other polymers. The XG solutions with small concentration ($c = 10$ ppm, empty circles) showed no loss of efficiency, suggesting that molecular degradation does not play an important role in these solutions. In fact, what is more curious is that the loss of

efficiency appears when the concentration is increased (empty squares). Clearly, the period of time in which the maximum level of DR is maintained falls with increasing concentration (t_r = 90s with c = 10 ppm and t_r = 3s with c = 50 ppm). Such effect is also noted when is used seawater as a solvent. We can see a very low level of drag reduction (DR < 0,05, full symbols) and any efficiency loss in this conditions.

Fixing again the temperature (25ºC) and Reynolds number (1360), Figure 6 shows de effect of synthetic sea salt concentration on drag reduction against time, in solutions of PEO, PAM, and XG , c = 50ppm. We tested different concentrations of salt: SSW 10ppm (10 ppm by weight of synthetic sea water, only for XG), SSW (3,5% by weight of synthetic sea water), and SSW10% (10% by weight)
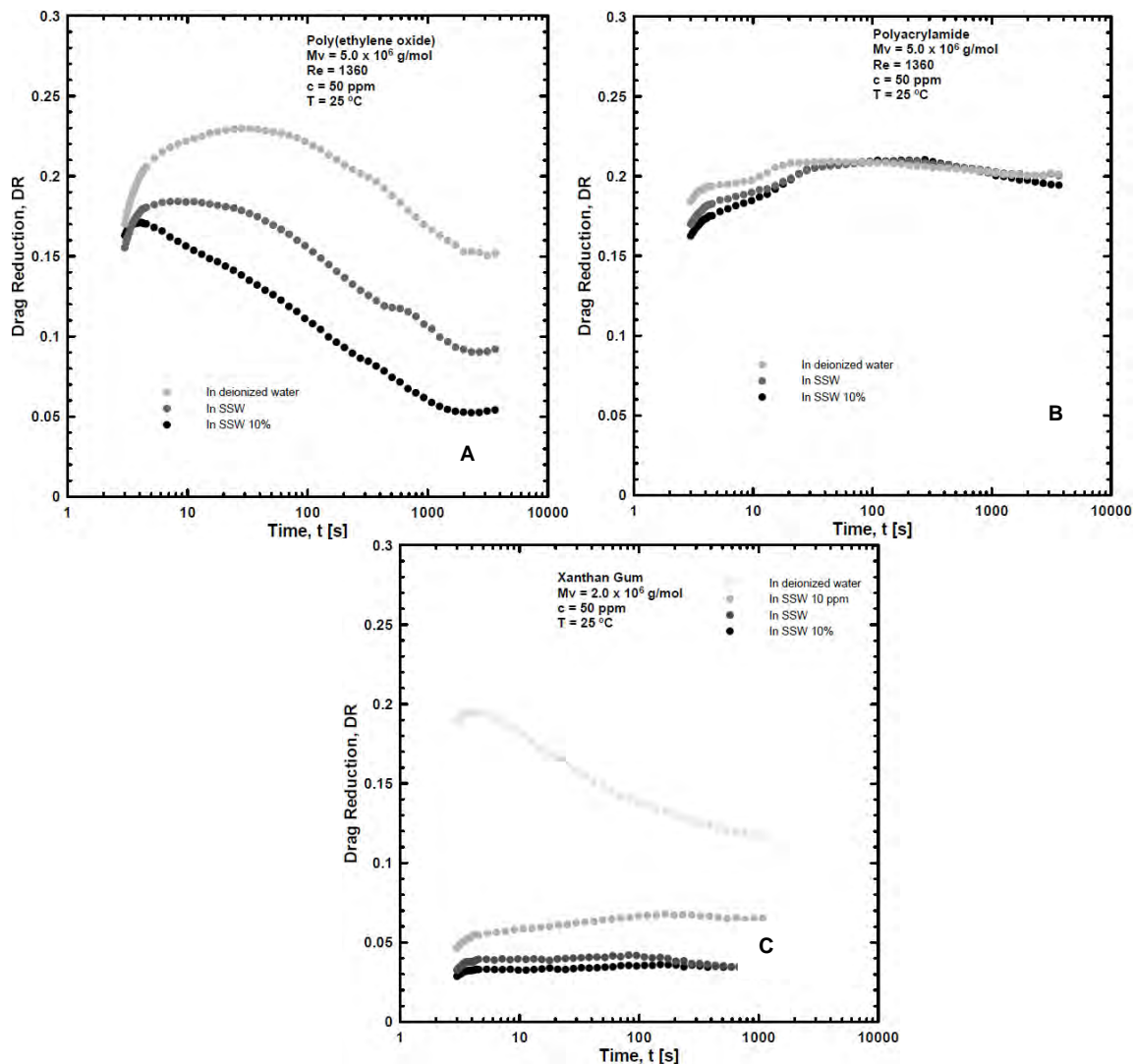

Figure 6. Effect of synthetic sea salt concentration on DR as a function of time.

We can note a great influence of salt concentration on the drag reduction by PEO. As verified in friction factor analyses and by Elbing et al. (2009) and Kamel et al. (2009), DR is lower in salt solutions. We can clearly see that t_r and DR_{asy} are decrease with increasing synthetic sea salt concentrations, indicating that polymer degradation is more pronounced under such conditions. In Figure 6 B the addition of more amount of sea salt in PAM solutions does not cause no significant change on drag reduction. On the other hand, the XG solutions with salt are dramatically affected. Clearly DR_{max} falls from 0,20 to 0,07 (65% loss of efficiency) when just 10ppm of salt is present in the solution (SSW 10ppm) and falls from 0,07 to 0,04 in SSW (3,5% by weight of synthetic sea water). However the addition of more amount of salt (SSW 10%) does not cause more loss of efficiency. Again we can clearly note a great difference between the XG solutions with deionized water and seawater. Just 10ppm of sea salt (0,001%) can completely change the curve of drag reduction. The development time, resistance time, and asymptote time are no longer observed. Apparently the drag reduction starts at DR_{asy} in XG solutions with synthetic sea salt. We believe that such effect is related to the change of molecular structure of XG.

ISSN 2176-5480

Rafhael M. Andrade and Edson J. Soares
Drag Reduction in Seawater by Polymer Addition into a Rotating Cylindrical Double Gap Device

After a close examination of the drag reduction decay functions for each polymer, it is clear that each variable, Re, polymer concentration, and synthetic sea salt concentration plays a quite different role in the Xanthan Gum mechanism of drag reduction. As reported by Morris (1977) and Norton et al. (1984), at moderate temperatures and low ionic forces, XG presents a stable organized helical conformation resulting in a rigid molecular structure. Such an organized structure can be modified by increasing temperature or salinity. In such conditions, the ionic forces are altered and the helical configuration changes to a recoiled one. Supposedly, in this new configuration the Xanthan Gum's capability to reduce drag drops dramatically. However we can see such behavior also in Figure 5 C comparing different polymer concentration. Since the ionic forces increase with increasing polymer concentration, the helical form perhaps becomes unstable and part of the molecules changes its conformation to the tangled form at high concentrations. We suppose the change of configuration is intensified by the turbulence and a loss of efficiency is perceived. Hence, possibly, a great part of the loss of efficiency observed could be related to changes in the microstructure of the Xanthan Gum. In other words, the loss of efficiency in XG solutions is not related to the polymer degradation.

3.3 Relative drag reduction decay

The PEO results of the previous subsection, witch presented more clearly the influence of polymeric degradation, can be reorganized so as to be presented from the perspective of degradation using relative drag reduction, $DR' = DR(t)/DR_{max}$. Each curve is plotted from $DR'=1$ to its minimum value, DR'_{asy}, for sufficiently large time. The difference, $1 - DR'_{asy}$, is the reduction in the drag reduction caused by the scission of the molecules. Figure 7 displays the relative drag reduction against the time for a range of Reynolds number, polymer concentration, synthetic sea salt concentration in PEO solutions, $M_v = 5,0$ x 10^6 g/mol. The temperature was kept at 25ºC.
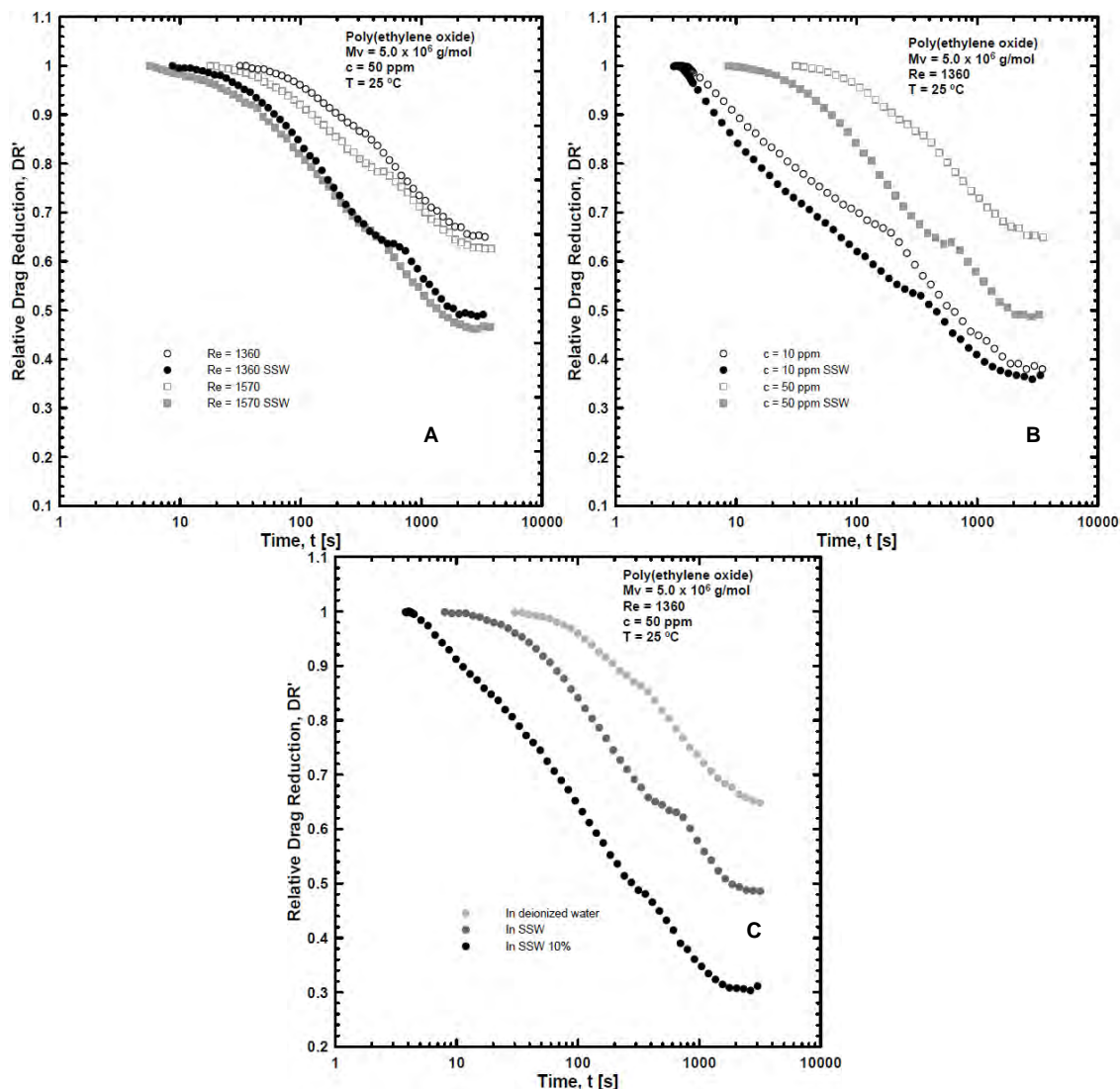

Figure 7. Effect of Reynolds number, polymer concentration, and synthetic sea salt concentration on DR'.

We can note that polymer degradation is more intense at higher Reynolds number and lower polymer concentration, as observed by Abernathy (1970), Moussa e Tiu (1994), Vanapalli et al. (2005) e Elbing, et al (2009) e Pereira e Soares (2012). Using the relative drag reduction analyze, we can note that synthetic sea salt plays an important role in polymer degradation. The PEO solutions with synthetic sea salt is more degraded than the others solutions. In Figure 7 C we can see 70% loss of efficiency when the salt concentration is 10% by weight (black circles), while PEO solubilized in deionized water (light gray circles) presents just 35% loss of efficiency. This effect is difficult to note when is just analyzed the friction factor as a function of the Reynolds number, as proceeded Elbing et al. (2009) and Kamel et al. (2009). Zakin and Hunston (1978) report that in a poor solvent mechanical degradation is more rapid than in a good solvent. Such results support our hypothesis that the addition of this synthetic sea salt becomes the deionized water a poor solvent for PEO.

4. FINAL REMARKS

We presented an experimental approach developed to analyze the drag reduction and polymer degradation in seawater by high–molecular weight polymers using a cylindrical double gap rheometer device. The tests were conducted with dilute solutions of Poly(ethylene oxide) (PEO), Polyacrylamide (PAM), and Xanthan Gum (XG) for a wide range of Reynolds number, polymer concentration, and synthetic sea salt concentration.

The results show that synthetic sea salt plays an important role in the friction factor behavior, drag reduction, and polymer degradation. We note that the onset of drag reduction is delayed in solutions with synthetic sea salt (Figure 3), mainly in PEO and XG solutions. In the presence of salt the values of the coefficient $1/\sqrt{f}$ are less pronounced. The drag reduction in PEO and XG solutions is also significantly affected. In PEO solutions with salt DR_{max}, DR_{asy}, and t_r clearly decrease (Figure 4 A, Figure 5 A, and Figure 6 A) and the degradation is more pronounced (Figure 7). Such effect is noted in other researches using poor solvents; therefore, we suppose that the addition of this synthetic sea salt become the deionized water a poor solvent for PEO. We highlight the interesting behavior of friction factor and drag reductions in XG solutions, witch behaves as a rigid polymer (type "B"). The results suggest that the loss of efficiency in XG solutions is mainly related to the change of its microstructure. This may be caused by the addition of synthetic sea salt (Figure 6C) or by the turbulence in high concentration solutions (Figure 4 C and Figure 5 C).

5. ACKNOWLEDGEMENTS

6. REFERENCES

Bewersdorff, H.W. and Berman, N.S., 1988 The influence of flow-induced non-Newtonian fluid proprerties on turbulent drag reduction, Rheologica Acta, vol. 27, pp. 130-136.

Bizoto, V. C. and Sabadini, E., 2008. Poly(ethylene oxide) x polyacrylamide. Journal of Applied Polymer Science, vol. 25, pp. 1844-1850.

Burger, E. D. and Chorn, L. G. , 1980. Studies of drag reduction conducted over a broad range of pipeline conditions when flowing prudhoe bay crude oil, J. Rheology, vol. 24, pp. 603.

Chakrabarti, S. B. Seidl, J. V. Brunn, P. O., 1991. Correlations between porous medium flow data and turbulent flow results for aqueous hydroxypropylguar solutions (part 2). Rheologica Acta, vol. 30, pp. 124-130.

Choi, H. J., Kim, C. A., Sohn, J., Jhon, M. S., 2001. An exponential decay function for polymer degradation in turbulent drag reduction. Carbohydrate Polymers, vol. 45, pp. 61-68.

Dimitropoulos, C. D.; Dubief, Y.; Shaqfeh, E. S. G.; Moin, P. and Lele, S. K. , 2005. Direct numerical simulation of polymer-induced drag reduction in turbulent boundary layer flow, Physics of Fluids, vol. 17, pp. 1–4.

Dubief, Y.; White, C. M.; Terrapon, V. E.; Shaqfeh, E. S. G.; Moin, P. and Lele, K. , 2004. On the coherent drag-reducing and turbulence-enhancing behaviour of polymers in wall flows, J. Fluid Mech, vol. 514, pp. 271–280.

Elbing, B. R. Solomon, M. J. Perlin, M. Dowling, D. R. and Ceccio, S. L., 2011. Flow-induced degradation of drag-reducing polymer solutions within a high-reynolds- number turbulent boundary layer, J. Fluid Mech, vol. 670, pp. 337–364.

Elbing, B. R.; Winkel,E. S.; Solomon, M. J and Ceccio, S. L., 2009. Degradation of homogeneous polymer solutions in high shear turbulent pipe flow, Exp Fluids, vol. 47, pp. 1033–1044.

Fabula, G., 1971. Fire-fighting benefits of polymeric friction reduction, Trans ASME J Basic Engng, pp. 93–453.

ISSN 2176-5480

Rafhael M. Andrade and Edson J. Soares
Drag Reduction in Seawater by Polymer Addition into a Rotating Cylindrical Double Gap Device

Flory, P. J., 1971. Principles of Polymer Chemistry. Cornell University Press, Ithaca,NY.

Golda, J., 1986. Hydraulic transport of coal in pipes with drag reducing additives. Chem Engng Commun, vol. 45, pp. 53-67.

Hershey, H. C. and Zakin, J. L., 1967. A molecular approach to predicting the onset of drag reduction in the turbulent flow of dilute polymer solutions, Chemical Engineering Science, vol. 22, pp. 184–187.

Hunston, D. L. and Zakin, J. L., 1980 Effect of molecular parameters on the flow rate dependence of drag reduction and similar phenomena, Progress in Astronautics and Aeronautics, vol. 72, pp. 373–385.

Jaafar, J. Escudier, M. P. and Poole, R. J., 2009 Turbulent pipe flow of a drag-reducing rigid rod-like polymer solution, Journal of Non-Newtonian Fluid Mechanics, vol. 161, pp. 86–93.

Kalashnikov, V. N., 1998. Dynamical similarity and dimensionless relations for turbulent drag reduction by polymer additives, Journal of Non-Newtonian Fluid Mechanics, vol. 75, pp. 209–230.

Kalashnikov, V. N., 2002. Degradation accompanying turbulent drag reduction by polymer additives. Journal of Non-Newtonian Fluid Mechanics, vol. 103, pp. 105-121.

Kamel, A.; Shah, S. N., 2009 Effects of salinity and temperature on drag reduction characteristics of polymers in straight circular pipes, Journal of Petroleum Science and Engineering, vol. 67, pp. 23–33.

Kim, C. A., Lee, K., Choi, H. J., Kim, C. B., Kim, K. Y., Jhon, M. S., 1985. The turbulent drag reduction by graft copolymers of guar gum and polyacrylamide. Journal of Applied Polymer Science, vol. 31, pp. 4013-4018.

Lumley, J. L., 1973. Drag reduction in turbulent flow by polymer additives. j. polym, Journal of Polymer Science Macromolecular Reviews, vol. 7, pp. 263–290.

Moussa, T. and Tiu, C., 1994. Factors aafecting polymer degradation in turbulent pipe flow, Chemical Engineering Science, vol. 49, pp. 1681–1692.

Morris, E.R., 1977 Molecular Origin of Xanthan Solution Properties, Extracellular Microbial Polysaccharides, ACS Symposium Series, Chapter 6, vol. 45, pp. 81-89.

Nakken, T. Tande, M. and Elgsaeter, A. , 2001. Measurements of polymer induced drag reduction and polymer scission in taylor flow using standard double-gap sample holders with axial symmetry, Journal of Non-Newtonian Fluid Mechanics, vol. 97, pp. 1–12.

Norton, I.T. Goodall, D.M. Frangou, S.A. Morris, E.R and Ress, D.A., 1984 Mechanism and dynamics of conformational ordering in xanthan polysaccharide, Journal of Molecular Biology, vol. 175, pp. 371-394.

Paterson, R. W., Abernathy, F., 1970. Turbulent flow drag reduction and degradation with dilute polymer solutions. J. Fluid Mech, vol. 43, pp. 689-710.

Pereira, A. S. and Soares, E. J. , 2012. Polymer degradation of dilute solutions in turbulent drag reducing flows in a cylindrical double gap rheometer device, Journal of Non-Newtonian Fluid Mechanics, vol. 179, pp. 9–22.

Sohn, J. I. Kim, C. A. Choi, H. J. and Jhon, M. S. , 2001. Drag-reduction effectiveness of xanthan gum in a rotating disk apparatus, Carbohydrate Polymers, vol. 45, pp. 61–68.

Tabor, M. and Gennes, P. G. D., 1986. A cascade theory of drag reduction, Europhysics Letter, vol. 7, pp. 519–522.

Vanapalli, S. A. Islam, T. M. and Solomon, J. M., 2005. Universal scaling for polymer chain scission in turbulence, Physics of Fluids, vol. 17.

Virk, P. S. Mickley, H. S. and Smith, K. A., 1967. The toms phenomenom: turbulent pipe flow of dilute polymer solutions, Journal of Fluid Mechanics, vol. 22, pp. 22–30.

Virk, P. S., 1975a. Drag reduction fundamentals, AIChE Journal, vol. 21, pp. 625–656.

Virk, P. S., Sherman, D. C.,Wagger, D. L., 1997. Additive equivalence during turbulent drag reduction. AIChE Journal, vol. 43, pp. 3257-3259.

White, C. M. and Mungal, M. G., 2008. Mechanics and prediction of turbulent drag reduction whit polymer additives, Annual Review of Fluid Mechanics, vol. 40, pp. 235–256.

Zakin, J. L. and Hunston, D. L., 1978 Effects of solvent nature on the mechanical degradation of high polymer solutions, Journal of Applied Polymer Science, vol. 22, pp. 1763–1766.

7. RESPONSIBILITY NOTICE

The authors are the only responsible for the printed material included in this paper.